COBEM 2023 27TH INTERNATIONAL CONGRESS OF MECHANICAL ENGINEERING

ABCM Brazilian Society of Mechanical Sciences and Engineering
27th ABCM International Congress of Mechanical Engineering
December 04-08, 2023, Florianópolis-SC, Brazil

COB-2023-0706
ANALYSIS OF ELECTROOSMOTIC FLOW IN MICROCHANNELS THROUGH INTEGRAL TRANSFORMS

Waneise Caroline Oliveira de Souza
João Nazareno Nonato Quaresma
Emanuel Negrão Macêdo
Helder Kiyoshi Miyagawa
School of Chemical Engineering, Federal University of Pará, Belém, PA, Brazil
souzawaneise@gmail.com, quaresma@ufpa.br, enegrao@ufpa.br, helderkm@ufpa.br

Bruno Marques Viegas
Faculty of Biotechnology and Bioprocess Engineering, Federal University of Pará, Belém, PA, Brazil
bviegas@ufpa.br

Renato Machado Cotta
Laboratory of Transmission and Technology of Heat, Mechanical Engineering Department, POLI & COPPE/UFRJ, Federal University of Rio de Janeiro, Rio de Janeiro, RJ, Brazil
Navy Research Institute, IPqM-CTMRJ, General Directorate of Nuclear and Technological Development, DGDNTM, Brazilian Navy, Rio de Janeiro, RJ, Brazil
cotta@mecanica.coppe.ufrj.br

Arman Sadeghi
Department of Mechanical Engineering, University of Kurdistan, Sanandaj 66177-15175, Iran
a.sadeghi@eng.uok.ac.ir

Abstract. *This work presents a hybrid numerical-analytical solution through the Generalized Integral Transform Technique (GITT) for electroosmotic flow of an electrolyte solution in rectangular microchannels with the use of polyelectrolyte (PEL) grafted brushes of uniform properties in the wall-channel region. The governing equations are derived from the direct application of the basic equations of electrokinetic forces and momentum conservation considering steady fully developed flow, uncharged walls, constant PEL thickness, and the same permittivity and viscosity inside and outside the grafted layer. The GITT solution is obtained by applying the single domain formulation for modeling both the inside and outside of the PEL layer, which leads to a fully analytical solution for the electric potential field and a hybrid solution of the momentum equation. The results obtained are in excellent agreement with those in the literature. Also, an analysis of the governing parameters is performed to observe the effects on the electrical potential and velocity fields.*

Keywords: *Electroosmotic flow, Grafted microchannels, Hybrid solutions, Integral transforms.*

1. INTRODUCTION

Electro-kinetics is a phenomenon that occurs when two electrically charged phases move relative to each other. This movement is established in the presence of a driving force which may be mechanical or electrical in nature. It has been widely studied in the development of new microfluidic devices capable of performing chemical and biomedical processes such as sample separation, DNA analysis, and drug discovery and delivery (Azari et al., 2020; Sadeghi, 2018). Electroosmosis, which is one of the main electrokinetic phenomena, occurs when ionic liquids encounter charged surfaces under the effect of an external electric field. This phenomenon occurs due to the attraction of surface charges by the opposite charges in the solution, creating a region with net charge density in the liquid near the wall, known as the electrical double layer (Azari et al., 2020).

To transport biofluids in microfluidic devices, it is necessary to mathematically characterize the transport mechanism for the efficient design of analytical systems (Peralta et al., 2018). The usual electrokinetic transport phenomena modeling depends on the assumption that fluid particles have no internal structure, for instance, assuming a Newtonian fluid behavior. However, microfluidic equipment often handles fluids of complex structure, such as polymer suspensions, liquid crystals, colloids, animal blood, lubricants, cell suspensions, chemicals, and drugs (Siva et al., 2021). The thermal transport characteristics of fully developed electroosmotic flow of such fluids in a slit microchannel with constant wall heat fluxes were investigated by (Sadeghi et al., 2011). Other authors performed an analysis of hydrodynamic dispersion

with fully developed electroosmotic flow of PTT viscoelastic fluids in low zeta potential slit microchannels (Hoshyargar et al., 2018).

In some electroosmotic flow applications, polyelectrolyte layers (PELs) are applied to cover the channel inner surface in lab-on-a-chip (LOC) platforms, providing smart cushioning and controllable physical and chemical properties (Gaikwad et al., 2020). PEL deposition allows for enhanced functionalities and controllable flows under an external electric potential (Das et al., 2015). The modeling of electroosmotic flow grafted with PEL brushes include the fully developed electroosmotic flow situation (Sadeghi, 2018), soft microchannels at high grafting densities (Sadeghi et al., 2019), electroosmotic mixing (Gaikwad et al., 2020), and rotational electroosmotic flow of viscoplastic materials (Patel et al., 2021). Recent studies on electroosmotic flow (EOF) with PEL use analytical solutions for calculating the electric potential and the velocity fields. However, for more complex problems with non-linear effects and complex geometries, traditional numerical methods are employed. An alternative method, the Generalized Integral Transform Technique (GITT), based on orthogonal eigenfunction expansions, has been demonstrated in solving EOF, such as in the pseudo-transient convection in microchannels with electroosmotic flow (Soares et al., 2008), and heat transfer in parallel-plate micro-channels with combined electroosmotic and pressure driven flows (Sphaier, 2012a, 2012b; Braga Jr and Sphaier, 2014).

In this work, electroosmotic flow in a microchannel of rectangular geometry, with the presence of PEL brushes (special charged polymer brushes) on its inner wall and with the development of the electrostatic potential, is investigated. The electric potential field is analytically integrated, and the velocity field is solved by the Generalized Integral Transform Technique (GITT) (Cotta, 1990, 1993; Cotta et al., 2016, 2017, 2018, 2023; Chen et al., 2022), which offers a robust solution, with low computational cost and controlled relative errors. Results are presented to illustrate the convergence behavior of the GITT solution for different governing parameters.

2. PROBLEM FORMULATION

The proposed model is based on the phenomenon of electroosmosis within the flow of a liquid with constant polyelectrolyte properties. In electroosmotic flows, the momentum equations contain a body force term to model the interactions between the free ions in the solution and the electrical field. The model here adopted considers fully developed flow of a liquid containing a symmetric solution of ions. The flow was divided into two regions, the first being the internal region of the ion flow along the channel and the second one being face-coated with the polyelectrolyte layer (PEL) of thickness t^*. It is assumed that the flow is steady and fully developed with uncharged microchannel walls, constant PEL thickness, and the same permittivity and viscosity at both inside and outside of the grafted layer (Fig. 1). Moreover, a low grafting density is considered, and the volumetric density of the charges is assumed low enough to permit utilizing the Debye-Huckel linearization (Sadeghi, 2018). Therefore, the electrical potential and the momentum equations are presented in dimensionless form as:

$$\frac{\partial^2\psi}{\partial y^2}+\frac{\partial^2\psi}{\partial z^2}-K^2\psi+\frac{K^2}{\eta_\lambda^2}\mathrm{N}=0, \qquad \frac{\partial^2 u}{\partial y^2}+\frac{\partial^2 u}{\partial z^2}-\alpha^2 f u+K^2\psi=0, \qquad 0<y<1,\ 0<z<W \tag{1a,b}$$

where the various dimensionless parameters in Eqs. (1) are defined as: $y=y^*/H^*$, $z=z^*/H^*$, $t=t^*/H^*$, $W=W^*/H^*$, $\psi=eZ_E\psi^*/(k_BT^*)$, $K=H^*/\lambda_E$, $\eta_\lambda=\lambda_{PEL}/\lambda_E$, $N=N^*/N^*_{PEL}$, $u=-eZ_E\mu u^*/(\varepsilon k_BT^*E_x)$, $\alpha=H^*(f^*_{PEL}/\mu)^{1/2}$, $f=f^*/f^*_{PEL}$. Here f, K, N, u, y, z, α, and ψ are the dimensionless forms representing the friction coefficient, the EDL thickness, the number density of PEL, axial velocity component, y coordinate, z coordinate, PEL friction factor, and the electrical potential, respectively. The corresponding boundary conditions are:

$$\left.\frac{\partial\psi}{\partial y}\right|_{y=0}=0,\left.\frac{\partial\psi}{\partial y}\right|_{y=1}=0,\left.\frac{\partial u}{\partial y}\right|_{y=0}=0,u|_{y=1}=0,\left.\frac{\partial\psi}{\partial z}\right|_{z=0}=0,\left.\frac{\partial\psi}{\partial z}\right|_{z=W}=0,\left.\frac{\partial u}{\partial z}\right|_{z=0}=0,u|_{z=W}=0 \tag{2a-h}$$

To consider the PEL/electrolyte boundary in the inner part of the microchannel, with the use of the single domain reformulation (Knupp et al., 2012; Cotta et al., 2016), N and f can be defined as:

$$N=f=\begin{cases}0, & \text{for } 0<y<1-t, 0<z<W-t\\ 1, & \text{otherwise}\end{cases} \tag{3a-b}$$

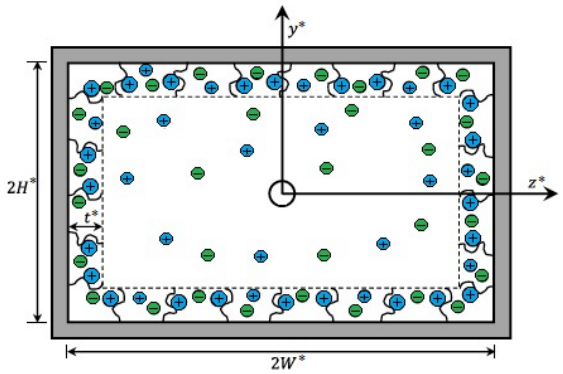

Figure 1. Schematic representation of the electroosmotic flow in the rectangular microchannel.

3. SOLUTION METHODOLOGY

Equations (1) are coupled, since the velocity depends on the electrical potential field, besides the coupling through the drag force created by the polyelectrolyte brushes. The Generalized Integral Transform Technique is now employed in the solution of this coupled linear PDE system. The application of this hybrid methodology will be presented in two parts, according to the availability of an analytical solution, as shown below.

3.1 Electrical potential field

Following the GITT formalism (Cotta, 1990,1993), an eigenvalue problem is chosen, which will offer the basis for the eigenfunction expansion of the electrical potential, namely:

$$\frac{d^2\Omega_i}{dy^2} + \beta_i^2 \Omega_i = 0 \tag{4}$$

$$\Omega_i'(0) = 0, \quad \Omega_i'(1) = 0 \tag{5a,b}$$

where the eigenvalues β_i and the eigenfunctions $\Omega_i(y)$ are given by:

$$\Omega_i(y) = \cos(\beta_i y), \qquad \beta_i = (i-1)\pi, \qquad i = 1, 2, 3, \ldots \tag{6a,b}$$

This eigenvalue problem enjoys the following orthogonality property:

$$\int_0^1 \Omega_i(y)\Omega_j(y)dy = \begin{cases} 0, & \text{for } i \neq j \\ M_i, & \text{for } i = j \end{cases}, M_i = \int_0^1 \Omega_i^2(y)dy = \begin{cases} 1, & \text{for } i = 1 \\ \frac{1}{2}, & \text{for } i > 1 \end{cases}, \quad \tilde{\Omega}_i(y) = \Omega_i(y)/\sqrt{M_i} \tag{7a-c}$$

where M_i and $\tilde{\Omega}_i(y)$ are the normalization integral and the normalized eigenfunctions, respectively. The eigenvalue problem given by Eqs. (4) and (5) allows for the definition of the following integral-transform pair:

$$\bar{\psi}_i(z) = \int_0^1 \tilde{\Omega}_i(y)\psi(y,z)dy, \text{ transform} \tag{8}$$

$$\psi(y,z) = \sum_{i=1}^{\infty} \tilde{\Omega}_i(y)\bar{\psi}_i(z), \text{ inverse} \tag{9}$$

Now, the integral transformation of the partial differential equation for the electrical field is performed. For this purpose, Eqs. (1a) and (2e,f) are operated on with $\int_0^1 \_\_\_\tilde{\Omega}_i(y)dy$ and after substituting the inverse formula given by Eq. (9), one obtains:

$$\frac{d^2\bar{\psi}_i}{dz^2} - \gamma_i^2\bar{\psi}_i = \bar{g}_i(z) \tag{10}$$

$$\left.\frac{d\bar{\psi}_i}{dz}\right|_{z=0} = 0, \quad \left.\frac{d\bar{\psi}_i}{dz}\right|_{z=W} = 0 \tag{11a,b}$$

where, $\gamma_i^2 = \beta_i^2 + K^2$, and

$$\bar{g}_i(z) = \begin{cases} \bar{g}_{1i}, & \text{for } 0 < z < W - t \\ \bar{g}_{2i}, & \text{for } W - t < z < W \end{cases}, \quad \bar{g}_{1i} = \begin{cases} \frac{-K^2 t}{\eta_\lambda^2}, & \text{for } i = 1 \\ \frac{K^2}{\eta_\lambda^2}\frac{\sqrt{2}}{\beta_i}(-1)^i \sin(\beta_i t), & \text{for } i > 1 \end{cases}, \quad \bar{g}_{2i} = \begin{cases} \frac{-K^2}{\eta_\lambda^2}, & \text{for } i = 1 \\ 0, & \text{for } i > 1 \end{cases} \tag{12a-c}$$

Equations (10) and (11) are analytically solved to furnish the following expressions for the transformed electrical potentials at the inner and outer regions respectively:

$$\bar{\psi}_{1i}(z) = -\frac{\bar{g}_{1i}}{\gamma_i^2}\left[1 - \frac{\sinh(\gamma_i t)}{\sinh(\gamma_i W)}\cosh(\gamma_i z)\right] - \frac{\bar{g}_{2i}}{\gamma_i^2}\frac{\sinh(\gamma_i t)}{\sinh(\gamma_i W)}\cosh(\gamma_i z), \qquad 0 < z < z_t \tag{13}$$

$$\bar{\psi}_{2i}(z) = -\frac{\bar{g}_{i1}}{\gamma_i^2}\sinh(\gamma_i z_t)\frac{\cosh[\gamma_i(W-z)]}{\sinh(\gamma_i W)} - \frac{\bar{g}_{2i}}{\gamma_i^2}\left\{1 - \frac{\sinh(\gamma_i z_t)\cosh[\gamma_i(W-z)]}{\sinh(\gamma_i W)}\right\}, \qquad z_t < z < W \tag{14}$$

where z_t=W–t. Equations (13) and (14) were obtained by using the additional continuity boundary conditions $\psi_1|_{z=z_t} = \psi_2|_{z=z_t}$, $\left.\frac{\partial\psi_1}{\partial z}\right|_{z=z_t} = \left.\frac{\partial\psi_2}{\partial z}\right|_{z=z_t}$, which in terms of the transformed potentials are $\bar{\psi}_{1i}\big|_{z=z_t} = \bar{\psi}_{2i}\big|_{z=z_t}$, $\left.\frac{d\bar{\psi}_{1i}}{dz}\right|_{z=z_t} = \left.\frac{d\bar{\psi}_{2i}}{dz}\right|_{z=z_t}$. The introduction of Eqs. (13) and (14) into inverse formula given by Eq. (9) completes the solution for the electric potential field, $\psi(y,z)$.

3.2 Velocity field

We follow the GITT formalism for solving the velocity field, similarly to the solution of the electrical potential field, and, for this purpose, the following eigenvalue problem was chosen:

$$\frac{d^2\Gamma_i}{dy^2} + \lambda_i^2\Gamma_i = 0 \tag{15}$$

$$\Gamma_i'(0) = 0, \qquad \Gamma_i(1) = 0 \tag{16a,b}$$

where λ_i and $\Gamma_i(y)$ are the eigenvalues and the eigenfunctions, respectively. Problem defined by Eqs. (15) and (16) are analytically solved to give:

$$\Gamma_i(y) = \cos(\lambda_i y), \qquad \lambda_i = (2i-1)\pi/2, \qquad i = 1, 2, 3, \ldots \tag{17a,b}$$

The eigenvalue problem given by Eqs. (15) and (16) enjoys the following orthogonality property:

$$\int_0^1 \Gamma_i(y)\Gamma_j(y)dy = \begin{cases} 0, & \text{for } i \neq j \\ N_i, & \text{for } i = j \end{cases}, N_i = \int_0^1 \Gamma_i^2(y)dy = \frac{1}{2}, \quad \tilde{\Gamma}_i(y) = \Gamma_i(y)/\sqrt{N_i} \tag{18a-c}$$

where N_i and $\tilde{\Gamma}_i(y)$ are the normalization integral and the normalized eigenfunctions, respectively. The eigenvalue problem given by Eqs. (15) and (16) allows for the definition of the following integral-transform pair:

$$\bar{u}_i(z) = \int_0^1 \tilde{\Gamma}_i(y)u(y,z)dy, \text{ transform} \tag{19}$$

$$u(y,z) = \sum_{i=1}^{\infty} \tilde{\Gamma}_i(y)\bar{u}_i(z), \text{ inverse} \tag{20}$$

The integral transformation of the partial differential equation for the velocity field is now performed. Therefore, Eqs. (1b) and (2g,h) are operated on with $\int_0^1 \_\_\_\tilde{\Gamma}_i(y)dy$ and after substituting the inverse formula given by Eq. (20), it results:

$$\frac{d^2\bar{u}_i}{dz^2} - \lambda_i^2\bar{u}_i - \alpha^2\sum_{j=1}^{\infty} A_{ij}\bar{u}_j + K^2\sum_{j=1}^{\infty} B_{ij}\bar{\psi}_j = 0 \tag{21}$$

$$\left.\frac{d\bar{u}_i}{dz}\right|_{z=0} = 0, \quad \left.\frac{d\bar{u}_i}{dz}\right|_{z=W} = 0 \tag{22a,b}$$

where,

$$A_{ij} = \int_0^1 \tilde{\Gamma}_i(y)\tilde{\Gamma}_j(y)f(y,z)dy, \qquad B_{ij} = \int_0^1 \tilde{\Gamma}_i(y)\tilde{\Omega}_j(y)dy \tag{23a,b}$$

The average velocity is defined as

$$u_{av} = \frac{1}{W}\left[\int_0^W \int_0^1 u(y,z)dydz\right] \tag{24}$$

Introducing the inverse formula for the velocity field, given by Eq. (20), into Eq. (24), the expression for the average velocity is obtained as

$$u_{av} = \frac{1}{W}\left[\sum_{i=1}^{\infty} C_i D_i\right], \quad C_i = \int_0^1 \tilde{\Gamma}_i(y)dy, \quad D_i = \int_0^W \bar{u}_i(z)dz \tag{25a-c}$$

4. RESULTS AND DISCUSSION

A computational code was written in the Fortran 95/2003 programming language to obtain numerical results for the electrical potential and velocity fields. Equations (21) and (22) for the computation of the transformed potentials of the velocity field constitute a boundary value problem given by a coupled system of ordinary differential equations, which was solved by the DBVPFD subroutine from the IMSL Library (2018), and a prescribed tolerance of 10^{-5} was used for such computations.

A brief convergence analysis of the eigenfunction expansions is provided for both electrical potential and velocity fields, and for the average velocity as well. For such analysis, it has been considered the values of W=1, η_λ=2, K=2, t=0.1 and α=1. Table 1 shows the convergence behavior at the center of the microchannel (y=0, z=0) for both fields, considering a maximum truncation order of NT=50 in the expansions. One may observe that full convergence to within five significant digits is reached with NT=30 or lower, while the average velocity reaches full convergence to five digits with NT=20. Also, a comparison with the results from the variational calculus approach, based on the work of Sadeghi (2018), shows an excellent agreement. Based on this analysis, we shall consider a truncation order of NT=50 throughout the subsequent computations.

Table 1. Convergence behavior of the eigenfunction expansions for both the electrical potential and velocity fields at the center of the rectangular microchannel and of the average flow velocity.

NT	$\psi(0,0)$	$u(0,0)$	u_{av}
10	0.26616×10^{-1}	0.42101×10^{-1}	0.22124×10^{-1}
20	0.26622×10^{-1}	0.42107×10^{-1}	0.22126×10^{-1}
30	0.26621×10^{-1}	0.42108×10^{-1}	0.22126×10^{-1}
40	0.26621×10^{-1}	0.42108×10^{-1}	0.22126×10^{-1}
50	0.26621×10^{-1}	0.42108×10^{-1}	0.22126×10^{-1}
(Sadegui, 2018)	0.26621×10^{-1}	0.42109×10^{-1}	0.22127×10^{-1}

In Figures 2 and 3 are shown typical transient behaviors of the electrical potential and velocity fields, respectively, for selected parametric values. The present GITT results (solid lines) are in excellent agreement with those from (Sadeghi, 2018), in symbols, again confirming the consistency of the present results.

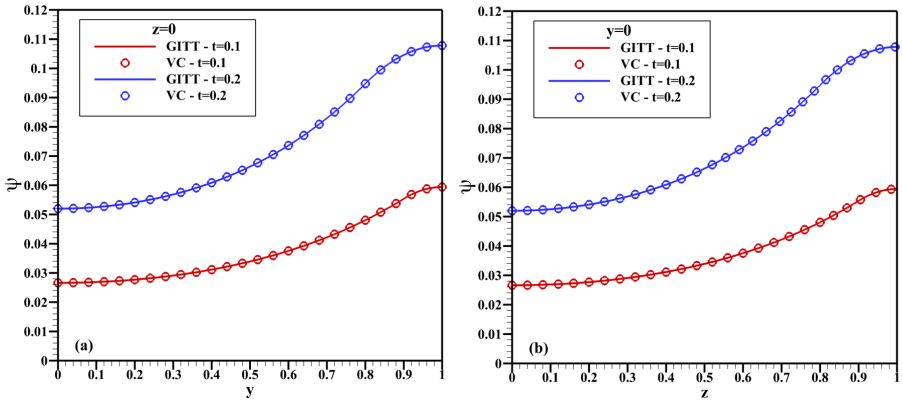

Figure 2. Comparison of the electrical potential field for t=0.1 and t=0.2.

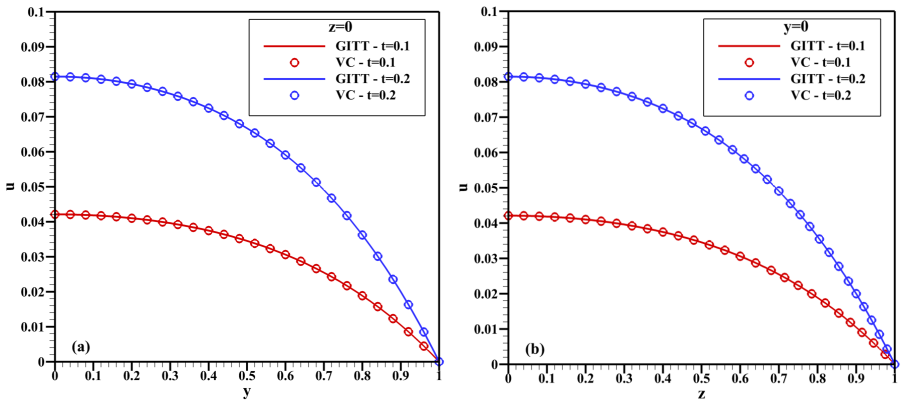

Figure 3. Comparison of the velocity field for t=0.1 and t=0.2.

A parametric analysis is now performed, based on the behavior of the electrical potential and velocity fields by considering different values of selected dimensionless governing parameters, i.e., α, η_λ, K, t and W. The base values were taken as α=1, η_λ=2, K=5, t=0.1, and W=2, unless the variation of one of these parameters is indicated. In Figures 4 are shown the effects of such governing parameters on the electrical potential distribution at the position z=0 and along the y-coordinate. Figure 4a shows the effect of the PEL thickness, where it is observed that as time increases, it leads to larger values in the distributions of the electrical potential since more charged ions are present in a wider region. An opposite effect is observed by increasing the values of the Debye length ratio (η_λ) in Figure 4b, mainly due to the presence of lower volumetric densities of fixed charges inside the PEL region with an increase of η_λ, for a fixed value of K. The increase of the Debye-Hückel parameter (K) results in larger values in the distributions of $\psi(y,0)$, particularly in the region near the wall microchannel (Figure 4c). This behavior is because higher K is related to thin EDL thickness, and the variation of the electrical potential is mainly close at the wall region, and uniform in the channel core. In Figure 4d, we depict the effects of increasing the dimensionless microchannel width, leading to lower values in the distributions for the electrical potential. For W=2 and 4, the distributions are practically coincident, indicating that from these values on there is no significant changes in the electrical potential field.

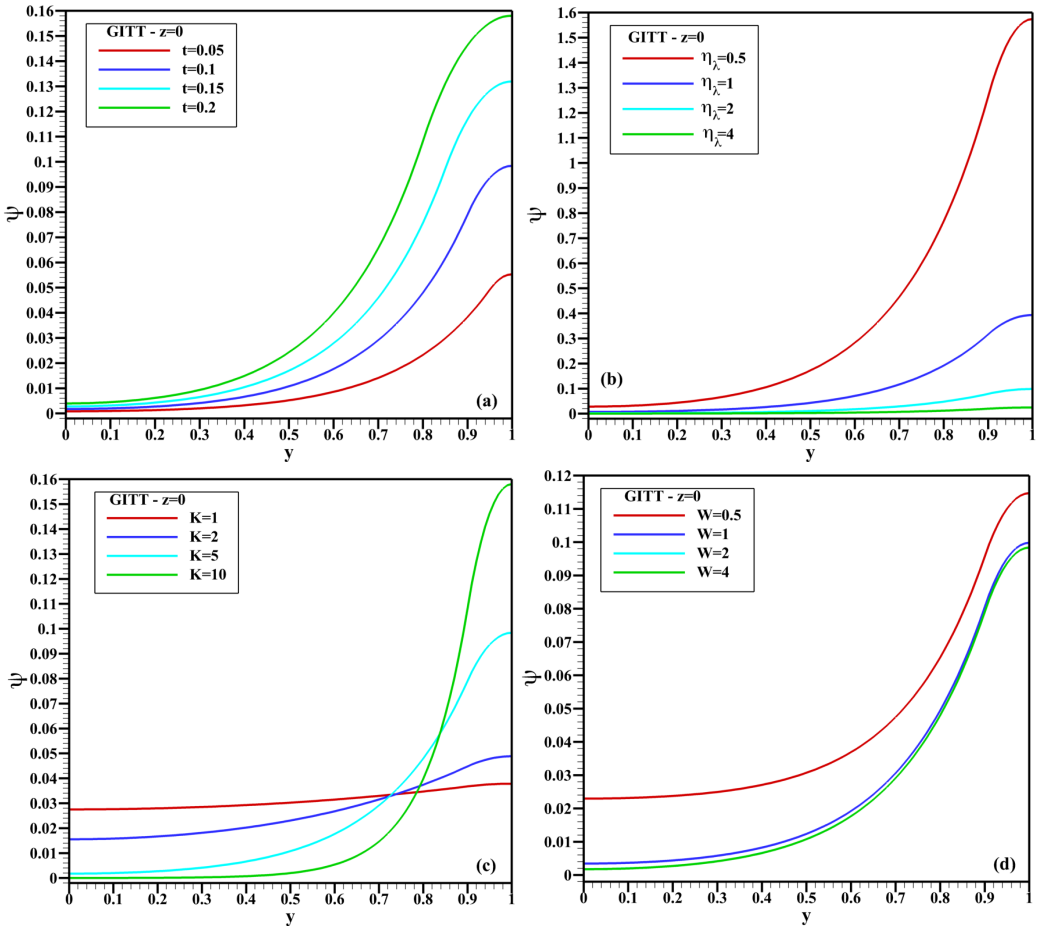

Figure 4. Influence of the governing parameters on the electrical potential distribution with base values α=1, η_λ=2, K=5, t=0.1, and W=2: (a) effect of t; (b) effect of η_λ; (c) effect of K; (d) effect of W.

In Figures 5 are shown similar analysis of the influence of the EOF governing parameters on the velocity distribution, again at the position z=0 and along the y-coordinate. Figure 5a shows the effect of the PEL thickness, where it is observed that for increasing time values result in larger values of the velocity since despite the thicker PEL layer that produces larger friction forces, the driving force in the charged region compensates such friction effect. Figure 5b evidentiates the opposite effect when increasing the values of the Debye length ratio (η_λ). For reasons pointed out in the discussion of Figure 4b, the increase of η_λ (with fixed K) decreases the values in the distribution of $\psi(y,0)$ and, consequently, decreases the values of $u(y,0)$. Since the increase of the K parameter leads to larger values of the electrical potential, the velocity distribution $u(y,0)$ is directly affected (Figure 5c). Figure 5d illustrates the effects of increasing the dimensionless microchannel width and merged distributions are verified in regions near the microchannel wall, while distinct values are found in the intermediate and central regions of the channel. The effect of the α parameter is shown in Figure 5e, where an increase of the dimensionless PEL friction factor (α) increases flow resistance, and lower levels in the velocity distribution are consequently found.

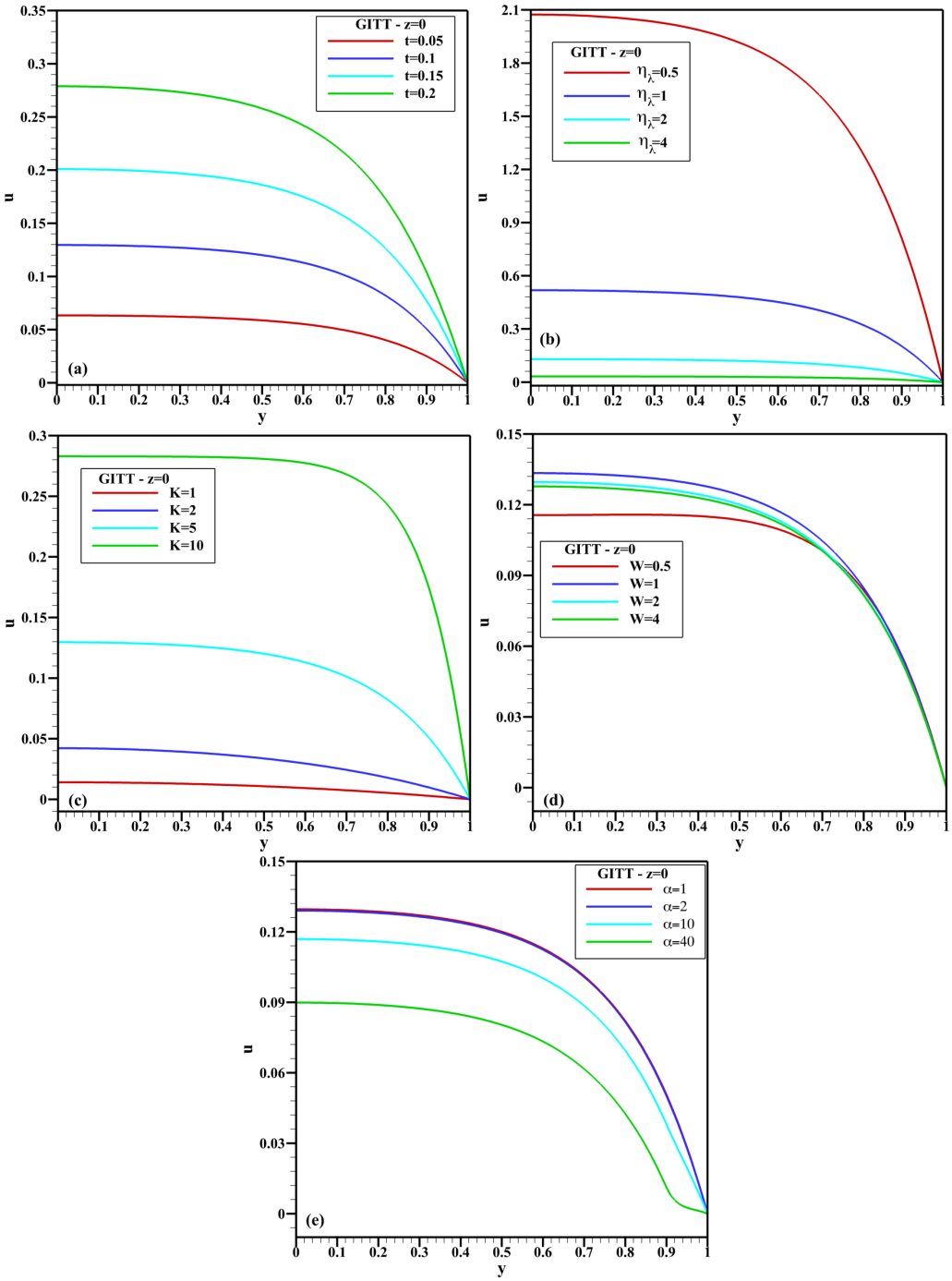

Figure 5. Influence of the governing parameters on the velocity distribution with base values α=1, η_λ=2, K=5, t=0.1, and W=2: (a) effect of t; (b) effect of η_λ; (c) effect of K; (d) effect of W; (e) effect of α.

5. CONCLUSIONS

The present work successfully applied the Generalized Integral Transform Technique (GITT) in the analysis of electroosmotic flow in rectangular microchannels with grafted walls. A convergence analysis of the proposed eigenfunction expansions is presented for both the electrical potential and velocity fields, besides the average velocity, with the achievement of impressive convergence rates. Also, comparisons of the present GITT results with those from variational calculus, Sadeghi (2018), were illustrated to reconfirm the effectiveness and consistency of the integral transform methodology here employed. An extensive parametrical analysis was performed to demonstrate the influence of the governing parameters on the electrical potential and velocity distributions. The proposed approach can be readily extended to more involved formulations and offers an interesting alternative solution path for more intensive computational tasks, such as in microfluidics optimization and properties identification through inverse problem analysis.

6. REFERENCES

Azari, M., Sadeghi, A., Chakraborty, S., 2020. "Electroosmotic flow and heat transfer in a heterogeneous circular microchannel". *Applied Mathematical Modelling*, Vol. 87, pp. 640–654.

Braga Jr, N.R. and Sphaier, L.A., 2014. "Analysis of conjugate heat transfer in microchannels: solution via hybrid analytical-numerical method". In *Proceedings of the ASME 2014 12th International Conference on Nanochannels, Microchannels, and Minichannels*. ICNMM2014. August 3-7, 2014, Chicago, Illinois, USA.

Chen, K., Cotta, R.M., Naveira-Cotta, C.P., Pontes, P.C., 2022. "Heat transfer analysis of compressible laminar flow in a parallel-plates channel via integral transforms". *International Communications in Heat and Mass Transfer*, Vol. 138, pp. 106368.

Cotta, R.M., 1990, Hybrid Numerical-Analytical Approach to Nonlinear Diffusion Problems, *Num. Heat Transfer, Part B*, Vol. 127, pp. 217-226.

Cotta, R.M., 1993. *Integral Transforms in Computational Heat and Fluid Flow*, CRC Press, Boca Raton.

Cotta, R.M., Knupp, D.C., Naveira-Cotta, C.P., 2016. *Analytical Heat and Fluid Flow in Microchannels and Microsystems*. Mechanical Eng. Series. Springer-Verlag.

Cotta, R.M., Knupp, D.C., and Quaresma, J.N.N., 2017, "Analytical Methods in Heat Transfer", In: Handbook of Thermal Science and Engineering, Vol.1, Chapter 2, pp.61-126, Francis A. Kulacki et al., Eds., Springer International Publ..

Cotta, R.M., Naveira-Cotta, C.P., Knupp, D.C., Zotin, J.L.Z., Pontes, P.C., Almeida, A.P., 2018. "Recent advances in computational-analytical integral transforms for convection-diffusion problems". *Heat and Mass Transfer/Waerme- und Stoffuebertragung*, Vol. 54, pp. 2475-2496.

Cotta, R.M., Lisboa, K.M., Naveira-Cotta, C.P., Quaresma, J.N.N., Knupp, D.C., and Sphaier, L.A., 2023, "Unified Integral Transforms with Non-Classical Eigenvalue Problems in Heat and Mass Transfer", *ASME J. Heat and Mass Transfer*, Review Article no.HT-22-1169, Vol. 145, no.1, 010801 pp.1-23.

Das, S., Banik, M., Chen, G., Sinha, S., Mukherjee, R., 2015. "Polyelectrolyte brushes: theory, modelling, synthesis and applications". *Soft Matter*, Vol. 11 (44), pp. 8550-8583.

Gaikwad, H.S., Kumar, G., Mondal, P.K., 2020. "Efficient electroosmotic mixing in a narrow-fluidic channel: the role of a patterned soft layer". *Soft Matter,* Vol. 16, pp. 6304-6316.

Hoshyargar, V., Talebi, M., Ashrafizadeh, S.N., Sadeghi, A., 2018. "Hydrodynamic dispersion by electroosmotic flow of viscoelastic fluids within a slit microchannel". *Microfluidics and Nanofluidics*, Vol. 22, pp. 1-15.

IMSL® Fortran Numerical Library, 2018. Version 2018, Rogue Wave Software Inc., Boulder, USA.

Knupp, D.C., Naveira-Cotta, C.P., and Cotta, R.M., 2012, "Theoretical Analysis of Conjugated Heat Transfer with a Single Domain Formulation and Integral Transforms", *Int. Comm. Heat & Mass Transfer*, Vol.39, no.3, pp.355-362.

Patel, M., Kruthiventi, S.S.H., Kaushik, P., 2021. "Polyelectrolyte layer grafting effect on the rotational electroosmotic flow of viscoplastic material". *Microfluidics and Nanofluidics*, Vol. 25, pp. 11:1-11:20.

Peralta, M., Bautista, O., Méndez, F., Bautista, E., 2018. "Pulsatile electroosmotic flow of a Maxwell fluid in a parallel flat plate microchannel with asymmetric Zeta potentials". *Applied Mathematics and Mechanics*, Vol. 39, pp. 667-684.

Sadeghi, A., 2018. "Theoretical modeling of electroosmotic flow in soft microchannels: a variational approach applied to the rectangular geometry". *Physics of Fluids*, Vol. 30, pp. 1-10.

Sadeghi, A., Saidi, M.H., Mozafari, A.A., 2011. "Heat transfer due to electroosmotic flow of viscoelastic fluids in a slit microchannel". *International Journal of Heat and Mass Transfer*, Vol. 54, pp. 17-18.

Sadeghi, A., Azari, M., Hardt, S., 2019. "Electroosmotic flow in soft microchannels at high grafting densities". *Physical Review Fluids*, Vol. 4, pp. 063701-1- 063701-23.

Siva, T., Jangili, S., Kumbhakar, B., 2021. "Heat transfer analysis of MHD and electroosmotic flow of non-Newtonian fluid in a rotating microfluidic channel: an exact solution". *Applied Mathematics and Mechanics*, Vol. 42, pp. 1047-1062.

Soares, P.O., Cotta, R.M., Silva Neto, A.J., 2008. "Convection in microchannels with electroosmotic flow: integral transforms in pseudo-transient formulation". In *Proceedings of the 12th Brazilian Congress of Thermal Sciences and Engineering ENCIT 2008*, Belo Horizonte, MG, Brasil.

Sphaier, L.A., 2012a. "Integral transform solution for heat transfer in parallel-plates micro-channels: combined electroosmotic and pressure driven flows with isothermal walls". *International Communications in Heat and Mass Transfer*, Vol. 39, pp. 769-775.

Sphaier, L.A., 2012b. "Analytical and hybrid solutions for heat transfer in combined electroosmotic and pressure-driven flows". In *Proceedings of the ASME 2012 10th International Conference on Nanochannels, Microchannels, and Minichannels ICNMM2012*. July 8-12, Rio Grande, Puerto Rico, USA.

7. RESPONSIBILITY NOTICE

The authors are the only responsible for the printed material included in this paper.